Acta Acustica 2024, **8**, 68

https://doi.org/10.1051/aacus/2024077

Available online at:
https://acta-acustica.edpsciences.org

Topical Issue – Active Noise and Vibration Control

SCIENTIFIC ARTICLE OPEN ACCESS

Optimizing a 2D active set-up for global control of low-frequency wall reflections in a semi-anechoic room

Emmanuel Friot[1,*], Cédric Pinhède[1], Philippe Herzog[2], and Romain Boulandet[3]

[1] Aix Marseille Univ, CNRS, Centrale Med, LMA UMR7031, Laboratoire de Mécanique et d'Acoustique, 4 Impasse Nikola Tesla, CS 40006 13453 Marseille Cedex 13, France
[2] ARTEAC-LAB, 29 rue Saint-Savournin, 13005 Marseille, France
[3] University of Applied Sciences and Arts Western Switzerland, Rue de la Prairie 4, 1202 Geneva, Switzerland

Received 29 April 2024, Accepted 31 October 2024

Abstract – Numerical simulations were carried out to optimize the design of an active semi-anechoic room. The active set-up includes control sources and microphones near the room ceiling and walls. The objective is to achieve global control, around an a priori unknown primary source, of the low-frequency wall reflections that are not adequately managed by absorbing material. The control strategy is based on the estimation, by linear filtering of total pressure signals, of the scattered pressure at minimization points meshing the room ceiling and walls. The required filters are identified off-line from measurements with a source whose radiation pattern is known. A 2D simple modal model is used to simulate active control in the frequency domain. The location of the minimization points, the set of estimation microphones and the method for computing the control signals from the measurements are varied. Simulations show that i) efficient global control of the scattered pressure can be achieved over a wide frequency band with a single non-smooth layer of minimization points, ii) accurate scattered pressure estimation at the minimization points can be achieved using usual pressure microphones distributed over all walls, iii) a Remote-Microphone technique seems slightly preferable to an Additional-Filter method for calculating the control signals.

Keywords: Active control, Wall scattering, Anechoic room

1 Introduction

Although the first theoretical studies on the active control of the acoustic field scattered by a surface date back to the 1950s ([1], chapter 9), it seems that such control has not yet been implemented outside the laboratory. Current studies on the subject focus either on cloaking to prevent object detection [2–6], possibly in water or soil, or on canceling the low-frequency reflections on the walls of anechoic rooms [7–10], for which an active semi-anechoic room demonstrator project is currently being carried out at the LMA.

The control system envisaged for the LMA room is based on estimating the wall-scattered sound pressure by linear filtering of total pressure measurements at a set of microphones close to the walls. The required filters are derived from the integral representation of the scattered field. They do not depend on the acoustic sources present and can therefore be identified off-line prior to real-time control. This overall control strategy was validated in real-time experiments [11, 12] and applied to the global control of low-frequency reflections from one wall [13]. The problem is now to apply it to the five absorbent walls of a small semi-anechoic room, combining this active technique for low frequencies with a traditional acoustic treatment for medium and high frequencies. Several numerical models of semi-anechoic rooms were developed and tested prior to the construction of the LMA demonstration room, in order to optimize transducer placement in terms of control efficiency, spatial extent and bandwidth, and to determine the complexity of the real-time algorithm and control processing unit required.

This paper presents three successive stages of numerical simulations conducted using a very simple 2D room model. The simulations have facilitated the design and optimization of the active system, and may also prove instructive for the global control of the scattered field in other situations. The initial objective of the simulations was to assess whether, with a given number of microphones and secondary sources, it was possible to control the scattered field in the 100–250 Hz frequency range in a small room. The second objective was to investigate whether estimation of the scattered field requires fully centralized computations from pressure measurements all over the walls, or whether

*Corresponding author: friot@lma.cnrs-mrs.fr

estimation using only a few measurements is possible. The third objective was to determine which of the two popular algorithms for control at virtual sensors allows the greater reduction of the scattered pressure in the semi-anechoic room case.

In order to meet these objectives the first stage of the simulations consisted in selecting the positions of a given number of control sources and minimization points which physically enable the scattered pressure to be controlled in the measurement zone of the semi-anechoic room, independently of the estimation of this scattered pressure. Previous experiments have shown that, with control sources on walls, as close as possible to the scattering surface, and minimization points nearby, global control of the wall scattered pressure is possible in practice [13]. This is why Boundary Pressure Control (BPC) [14], where the pressure is controlled on a surface for a global effect inside, was considered and simulated for the LMA room. However, in both theory and practice BPC control does not work at the resonant frequencies of the volume bounded by the control surface [15]. The numerical simulations presented here do indeed demonstrate the singularity of the BPC when using a microphone array meshing a regular surface, but it will be shown in particular how some irregularity of the minimization surface can regularize the control in practice, allowing the reduction of scattered pressure over a large area and a wide frequency band.

The second stage of the simulations consisted in comparing several processes of scattered pressure estimation. The control strategy studied here is based on estimating the scattered pressure at a set of minimization locations by means of appropriate linear filtering of the total pressure measured at a possibly different set of locations. Several strategies for reducing the number of microphones to be used have been compared, with a view to reducing the complexity of subsequent real-time control implementation. In particular, we assessed whether, for the same number of estimation microphones, it would be preferable to select them close to the estimation point or to distribute them over all the walls. It will be shown that accurate estimation of the scattered pressure at each minimization point requires total pressure measurements on all walls, but possibly in small numbers.

The estimation of the scattered pressure at a single point can be seen as a signal provided by a virtual microphone. The strategy studied here, which consists in filtering pressure measurements to estimate minimization signals, is similar to the Remote-Microphone (RM) technique [16] in the context of virtual sensing. In light of recent research, we have initiated a further stage of control simulations using the alternative Additional-Filter (AF) method [17, 18] for control at virtual microphones. The AF method consists in filtering the control signals which minimize the real sensor signals rather than filtering the real signals in order to obtain virtual error signals. In the case of the LMA room, with less control sources than sensors, AF requires in theory less linear filters than RM. In practice in real-time both methods require little specific computer memory if control is implemented using a Filtered-Error Least Mean Square (LMS) algorithm in place of a Filtered-reference LMS [12]. However, using AF could reduce the burden of collecting data to identify off-line the filters required to estimate scattered signals from real signals.

Section 2 of this paper briefly presents the theory of the proposed control strategy, the demonstration room built at LMA and a 2D model of the active control system. Section 3 deals with a practical regularization of BPC which leads to efficient control when the exact scattered pressure is used as minimization signal. Section 4 shows control results when scattered pressure estimates, instead of the exact scattered pressure, are used as minimization signals. Section 5 compares the AF and RM methods in the case of the active semi-anechoic room. Section 6 summarizes the results of the 2D simulations and presents the current status of testing in the LMA demonstration room.

2 Control theory and 2D modeling of an active semi-anechoic room

2.1 Overview of the control strategy

This section briefly summarizes the principles of the control strategy studied here. More details are given e.g. in [9].

Whatever the acoustic sources, Green's representation of pressure p_{sca} scattered from surface S is classically written, at point r and angular frequency ω, as a function of total pressure p over S:

$$p_{\text{sca}}(\mathbf{r},\omega) = \iint_S \left[G(\mathbf{r}|\mathbf{r}_0,\omega)\frac{\partial}{\partial n_0}p(\mathbf{r}_0,\omega) - p(\mathbf{r}_0,\omega)\frac{\partial}{\partial n_0}G(\mathbf{r}|\mathbf{r}_0,\omega)\right] \mathrm{d}S_0 \tag{1}$$

where $\frac{\partial}{\partial n_0}$ denotes the surface normal derivative and G is the acoustic Green's function for the propagation medium considered in the absence of surface S. The active control strategy considered here is based on the estimation of the scattered pressure, with an adequate array of K pressure microphones, using a discrete approximation of the surface integral:

$$p_{\text{sca}}(\mathbf{r},\omega) \simeq \sum_{k=1}^{K} g_k(\mathbf{r}|\mathbf{r}_k,\omega)p(\mathbf{r}_k,\omega). \tag{2}$$

Coefficients g_k, combinations of an a priori unknown Green's function and generalized impedances, *do not depend on the sources*. They can be identified off-line, from measurements with known sources, and then used with unknown sources. In the case of non-stationary noise sources, the estimation of scattered pressure from total pressure measurements can theoretically be non-causal. However, the direct wave from a source in the room reaches the microphones before the walls, thereby contributing to causality. In this paper, the control results will be given without causality constraints, as if we were considering pure tones.

In addition to measuring the total pressure, microphones can also mark positions where the scattered pressure

is estimated and minimized. If, in an anechoic room, the microphones cover all the walls, canceling the scattered pressure on this closed surface guarantees global control inside the surface except at the Dirichlet resonance frequencies of the volume bounded by the surface [15]. In the case of a semi-anechoic room, controlling with microphones in front of the walls and ceiling only, but not the floor, means controlling on the closed surface obtained by including the mirror images of the microphones with respect to the floor.

2.2 Construction and equipping of a semi-anechoic demonstration room

Figure 1 shows the $5.34 \times 4.22 \times 2.77$ m^3 room that was built at LMA for testing the control of low-frequency wall reflections. Loudspeakers are placed near the walls to cancel out the scattered field as close as possible to where it is generated. Off-the-shelf cheap loudspeakers were chosen for operation in the 100–400 Hz range. An array of microphones is positioned in front of the room walls. It provides the total pressure measurements needed to estimate the scattered pressure at each of the microphones. These estimates will be used as the active control minimization signals.

Once the active low-frequency control system has been developed and validated, sound-absorbing materials will be inserted between the wall sources and the microphones. The objective is to create a semi-anechoic room combining active control for low frequencies and traditional passive absorption for higher frequencies. Similarly, in an existing anechoic room, an active control system for low-frequency reflections could be installed with acoustic sources in the plenum, between the absorbing wedges and the walls, and an array of microphones positioned near the tips of the wedges. Note that an active system may significantly reduce the required size of the absorbing wedges in a given room.

2.3 2D low-frequency modeling of the room without absorbing material

Several numerical models were developed and used prior to equipping the room, allowing to specify the number and position of transducers to be used. As the controllability of an acoustic field depends on parameters such as the number of transducers per wavelength or the distance from the primary to the secondary sources, the global visualizations of the acoustic field provided by a 2D model are particularly useful for dimensioning an active control system. Therefore only simple 2D simulations of the semi-anechoic room are presented here, full 3D Finite Element Modeling having been used only to confirm the relevance of the dimensioning rules deduced from the 2D simulations [19].

The 2D model used for the simulations below is a 4.22×2.77 m^2 vertical cross-section of the room built at LMA whose third dimension is implicitly supposed infinite (instead of 5.34 m). In this cavity the pressure radiated in $\mathbf{r}$ by a source in $\mathbf{r}_0$, considered as a linear monopole with surface flow rate q, can be approximated as a finite sum

Figure 1. The LMA active set-up for controlling low-frequency wall reflections.

of N damped normal modes, including all the modes whose resonance frequency lies in the band of interest:

$$p(\mathbf{r},\mathbf{r}_0) = \rho c^2 j\omega q \sum_{n=0}^{N} \frac{\boldsymbol{\psi}_n^t(\mathbf{r})\boldsymbol{\psi}_n(\mathbf{r}_0)}{(\omega_n^2 + 2j\xi_n\omega_n\omega - \omega^2)\int_{\mathcal{S}} \boldsymbol{\psi}_n^2 d\mathcal{S}} \quad (3)$$

where ρ designates the air density and c the sound speed. In the absence of sound-absorbing material on the walls, the room is lightly damped, so the modes $\boldsymbol{\psi}_n$ and eigenfrequencies ω_n to be considered can be those of the cavity with rigid walls. The damping ratios ξ_n to be used in equation (3) were obtained using Finite Element Modeling (FEM), in which a real surface impedance constant with frequency, uniform on the walls, high but not infinite except for the floor, corresponding to an absorption coefficient of 10%, was taken as the boundary condition. Databases give a 2% a absorption coefficient for plaster at 100 Hz. However simulations with 2% gave unrealistic results above 200 Hz and measurements in the LMA demonstration room also showed more absorption at very low frequency because of wall vibrations. On the contrary, the model resulting from a 10% absorption coefficient led to simulated Frequency Response Functions similar to the measured ones.

In 2D, the pressure radiated by a monopole in a free field can be written as:

$$p_{\text{dir}}(\mathbf{r},\mathbf{r}_0) = \rho j\omega q \frac{-i}{4} H_0^{(2)}\left(\frac{\omega}{c}||\mathbf{r}-\mathbf{r}_0||\right) \quad (4)$$

where $H_0^{(2)}$ is the zero-order Hankel function of the second kind. The pressure scattered by the walls of a semi-anechoic room containing a monopole can finally be written taking into account the image source at $\mathbf{r}_0'$ of the monopole with respect to the room floor:

$$p_{\text{sca}}(\mathbf{r},\mathbf{r}_0) = p(\mathbf{r},\mathbf{r}_0) - p_{\text{dir}}(\mathbf{r},\mathbf{r}_0) - p_{\text{dir}}(\mathbf{r},\mathbf{r}_0'). \quad (5)$$

The 2D model allows fast computations but it has limitations, especially when compared to FEM:

- All of the sources within the model are monopoles, exhibiting near-field radiation that differs significantly from that observed around real loudspeakers.
- The room modes derived from the rigid case within the model are symmetric, whereas in a semi-anechoic room the pressure is observed to be lower in the vicinity of the walls than near the floor.

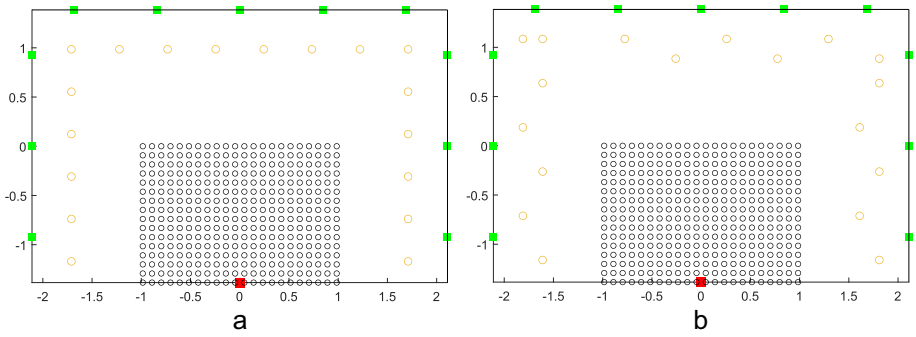

Figure 2. Two configurations for simulating the control of the acoustic pressure scattered by the walls of a semi-anechoic room: primary (monopole) source ■, control sources ■; scattered pressure sensors near the walls ○ and in the room measurement zone o.

- The simulations presented here use a constant absorption coefficient across frequencies. It would be more appropriate to derive the modal damping coefficients in the model from the complex modes of a FEM calculation, incorporating a frequency-dependent surface impedance on the walls.

The control simulations presented below are performed frequency by frequency without consideration of the causality constraint imposed in real-time active control. Consequently, optimal control is obtained directly by pseudo-inversion of the frequency response matrix between the control sources and the minimization microphones at each frequency.

3 Practical regularization of Boundary Pressure Control

In this section, we focus on the controllability of wall-scattered sound pressure inside a semi-anechoic room measurement zone, using sources and microphones close to the room walls, assuming the scattered pressure can be measured directly. Controlling an acoustic sound field by controlling the pressure at an enclosing array of microphones is usually referred to as Boundary Pressure Control (BPC) [14, 15].

Figure 2 shows two set-ups for 2D control simulations which differ only in the positions of the 18 microphones placed close to the walls. The set-up on the left, with microphones meshing a rectangular boundary, is the simplest to implement. The set-up on the right includes some irregularity in the arrangement of microphones near the walls. In both cases the primary source, whose sound scattered by the walls must be reduced, is located in the center of the room floor as is generally the case for the noise sources to be measured. Eleven monopole sources are placed on the walls and ceiling of the semi-anechoic room. Three hundred and fifty two points for calculating the pressure scattered by the walls are also considered to assess the effectiveness of global control in the room measurement zone.

Figure 3 shows as a function of frequency the Root-Mean-Square (RMS) value, without and with control, of the scattered pressure averaged over the 352 observation points in the measurement zone when the surface flow rate of the primary monopole placed in the room center is equal to 10^{-7} m^2/s at every frequency. Calculations for this and subsequent figures were performed from 20 to 400 Hz in steps of 0.1 Hz, truncating the summation in equation (3) after the first 91 modes with resonance frequency below 500 Hz.

The uncontrolled scattered pressure is at a high level, exhibiting notable resonances. Minimizing the scattered pressure at the 352 observation points with control sources results in high attenuation, not only at resonances. Further simulations showed that, below 250 Hz, the residual level of scattered pressure did not decrease with an increase in the number of sources. This residual scattered pressure is of no consequence at the output of the control computation, being merely a numerical aberration. Above 250 Hz, however, fluctuations in residual pressure are accompanied by a slight reduction in controllability, as observed with only 11 sources.

By minimizing the scattered pressure at the 18 microphones arranged in straight lines close to the walls, very good attenuation is also achieved on the 352 observation points up to 250 Hz, with the exception of a few isolated frequencies. The vertical dotted lines in Figure 3 indicate the Dirichlet resonance frequencies of the rectangle supporting the microphones and their image relative to the floor. It can be observed that the control exerted by the regular mesh of wall microphones is not optimal at certain frequencies, which is to be expected in the context of BPC [15].

By introducing some irregularity into the positions of the microphones, as shown in Figure 2 on the right, we can see that the theoretical singularity of global control has less influence on its performance in practice. As illustrated in Figure 2 on the right, the theoretical singularity of global control exerts a markedly diminished influence on its performance in practice when the microphones are more randomly arranged over the walls. One possible explanation is that out-of-alignment microphones pick up some information on the normal pressure gradient, given that the simultaneous cancellation of pressure and normal gradient on a closed surface guarantees cancellation inside, without any singular frequencies.

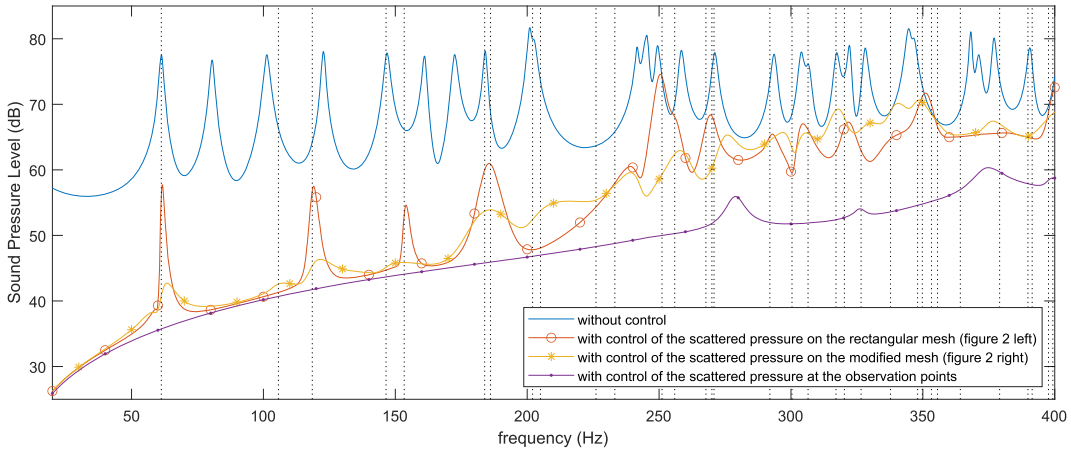

Figure 3. Spatial average of the RMS scattered acoustic pressure in the room measurement zone. The vertical dotted lines indicate the pressure-release eigenfrequencies of the rectangle enclosed by the microphones in Figure 2 left.

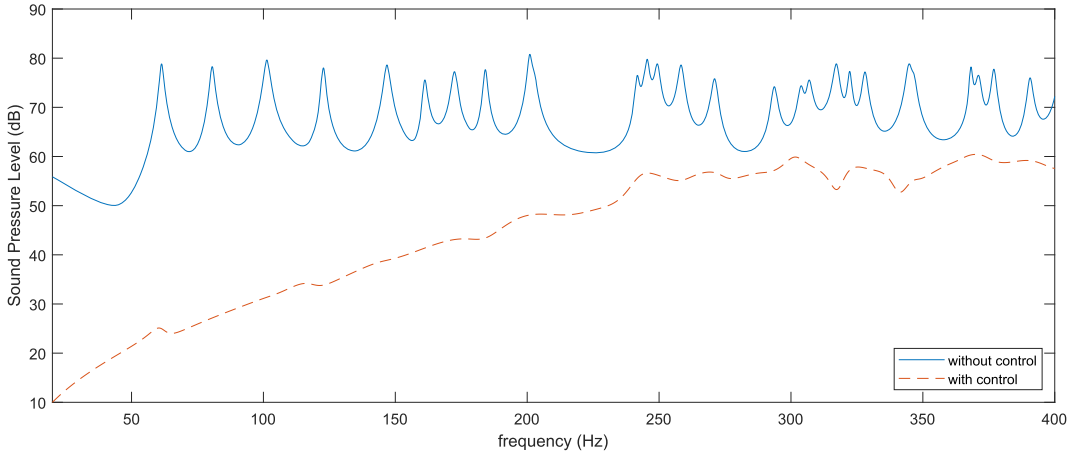

Figure 4. Spatial average of the RMS scattered acoustic pressure at the wall microphones with control of exact scattered pressure signals.

Finally, beyond 250 Hz, control at the wall microphones is still reducing the scattered pressure (up to 400 Hz) but it leads to less effective control in the center of the room than the one obtained by directly controlling pressure at the observation points. This shows that the sources are able to reduce the scattered field over the whole frequency range in the measurement zone but that the wall microphones are not anymore adequate minimization sensors for this above 250 Hz. Figure 4 displays the RMS scattered pressure averaged over the wall microphones shown in Figure 2 right. Although the noise reduction provided by active control decreases with frequency, the scattered pressure at the microphones is still significantly reduced in the 250–400 Hz band. Local control seems thus to be achieved but it does not imply global control above 250 Hz, for which more microphones would be required. In conclusion the source set-up seems to allow effective global control up to 400 Hz but the sensors only up to 250 Hz. With around 0.5 m between microphones, this corresponds to an order of magnitude of around 2 microphones per wavelength, which is quite usual in acoustic field sampling.

4 Control of scattered pressure estimates

4.1 Estimation of the scattered pressure using all the microphones

The control strategy studied here relies, as indicated by equation (2), on estimating the scattered pressure at minimization points by linear filtering of the total pressure measured at several points. As the operator in equation (1) mapping the total pressure to the scattered pressure close to the walls is independent of the acoustic sources, the coefficients g_k in equation (2) can be identified by placing a reference source in several locations [20], with known radiation in free field, allowing the simultaneous collection of the total pressure and the pressure scattered by the walls at several points. If $\mathbf{P}(\omega)$ and $\mathbf{P}_{\text{sca}}(\omega)$ denote matrices each column of which is respectively the vector of total and scattered pressures measured at angular frequency ω, then we can search for the matrix $\mathbf{G}(\omega)$ that minimizes the Frobenius norm:

$$J = ||\mathbf{P}_{\text{sca}}(\omega) - \mathbf{G}(\omega)\mathbf{P}(\omega)||^2_{\text{Fro}}. \tag{6}$$

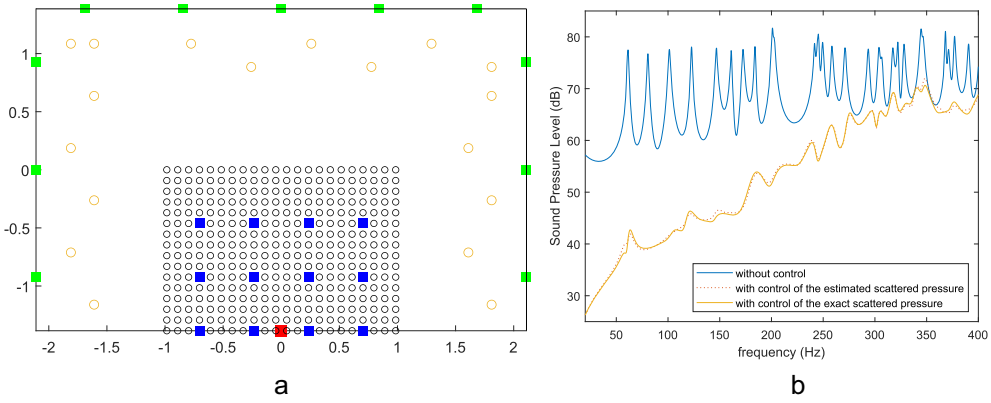

Figure 5. Set-up for the estimation of the scattered pressure, with reference source locations ■, and spatial average of the RMS scattered acoustic pressure in the room measurement zone with control of exact and estimated scattered pressure signals.

The solution to this inverse problem, possibly regularized if the number of reference source positions used is smaller than the number of measurement points, is a square matrix of dimension this number of measurement points. In practice, $\mathbf{G}(\omega)$ is easily obtained by pseudo-inversion or QR factorization of matrix $\mathbf{P}(\omega)$.

Figure 5 shows an active semi-anechoic room configuration for 2D simulation of the control of the wall scattered pressure estimated via total pressure filtering. A reference monopole is placed at 12 positions around the center of the room to generate the data needed to calculate at every frequency the 18×18 matrix $\mathbf{G}$ which maps the total pressure at all the microphones to the estimated scattered pressure at all the microphones. Figure 5 also shows the performance of the control when the *exact* scattered pressure or the *estimated* scattered pressure is minimized with a primary source placed at a position differing from those taken by the reference source. The performance of the two controls is very similar, emphasizing that the estimation of the scattered pressure from the 18 total pressure measurements is very good.

Further simulations showed that at least 8 positions were required for the reference source to be able to estimate the scattered pressure from the total pressure. With less positions the resulting estimation is poor, probably because not all the room degrees-of-freedom (i.e. the modes) are fully excited by the reference source. On the contrary, using more than 12 positions does not improve the estimation. With 8–12 positions, the inverse problem to solve appears to be quite well conditioned, leading to a robust computation of the scattered pressure estimator.

4.2 Estimation of the scattered pressure using selected microphones

In order to reduce the complexity of a future real-time control system, it may be advantageous to use only a subset of the microphones to estimate the pressure scattered at a single given location. We considered two options: either using a subset of microphones close to the estimation point, or using a few microphones evenly spaced over the whole wall surface From a numerical point of view, a simple way to obtain solution matrices of equation (6) with this type of constraint is to transform the equation whose unknown is a matrix into an equation whose unknown is a vector, which is easily written using the vectorization operator vec and the Kronecker product $\otimes$:

$$\begin{aligned} J(\omega) &= ||\mathbf{P}_{\text{sca}} - \mathbf{G}\mathbf{P}||_{\text{Fro}}^2 = ||\text{vec}(\mathbf{P}_{\text{sca}} - \mathbf{G}\mathbf{P})||_2^2 \\ &= ||\text{vec}(\mathbf{P}_{\text{sca}}) - (\mathbf{P}^t \otimes \mathbf{I}_m)\text{vec}(\mathbf{G})||_2^2 \end{aligned} \tag{7}$$

where $\mathbf{I}_m$ is the identity matrix of dimension the total number of microphones. The rows of this equation corresponding to zero coefficients in $\mathbf{G}$ can be removed and the non-zero components of the vector $\text{vec}(\mathbf{G})$ are easily obtained by pseudo-inversion of the matrix with the remaining columns of matrix $\mathbf{P}^t \otimes \mathbf{I}_m$. G is finally easily reconstructed by combining these components and the null coefficients.

Figure 6 compares the control performance obtained by estimating the scattered pressure on each of the 18 minimization microphones using the total pressure either:

- on all the 18 microphones,
- on the microphone where the scattered pressure is to be estimated and the 3 neighboring microphones on either side,
- on the microphone where the scattered pressure is to be estimated and 1 microphone out of 5 on either side.

In the first case, $\mathbf{G}$ is a full matrix with 324 coefficients and one scattered pressure is estimated from 18 signals. In the second case $\mathbf{G}$ is a matrix with 114 non-zero coefficients and one scattered pressure is estimated from 4 to 7 signals, depending on the position of the estimation point. In the third case $\mathbf{G}$ is a matrix with 82 non-zero coefficients and one scattered pressure is estimated from 4 or 5 total pressure signals. Although fewer signals are used in the third case than in the second, Figure 6 shows that estimating the scattered pressure with microphones on all the walls gives better results, particularly at very low frequencies, than estimating it with microphones close to the estimation points. This result is easily explained by the multiple reflections taking places: a wall reflects wavefronts that do not

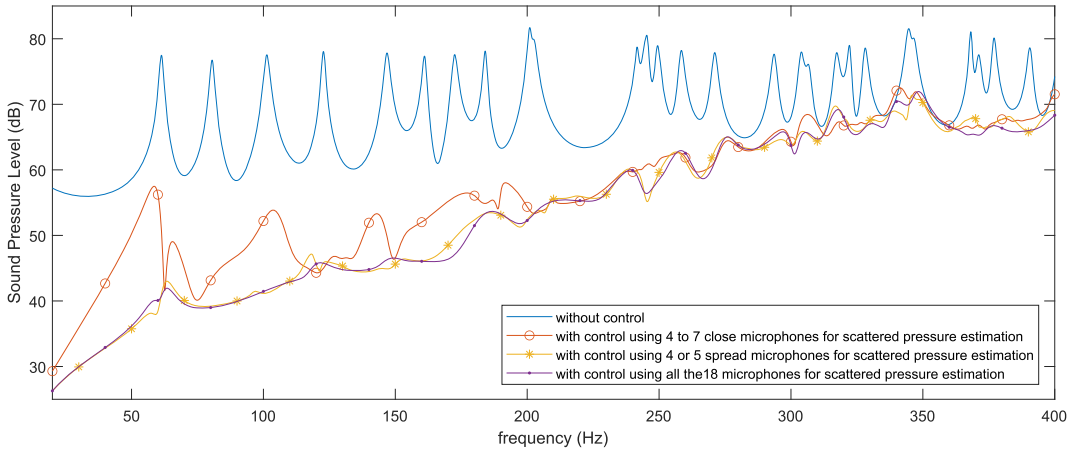

Figure 6. Spatial average of the RMS scattered acoustic pressure in the room measurement zone with control using various estimations of scattered pressure signals.

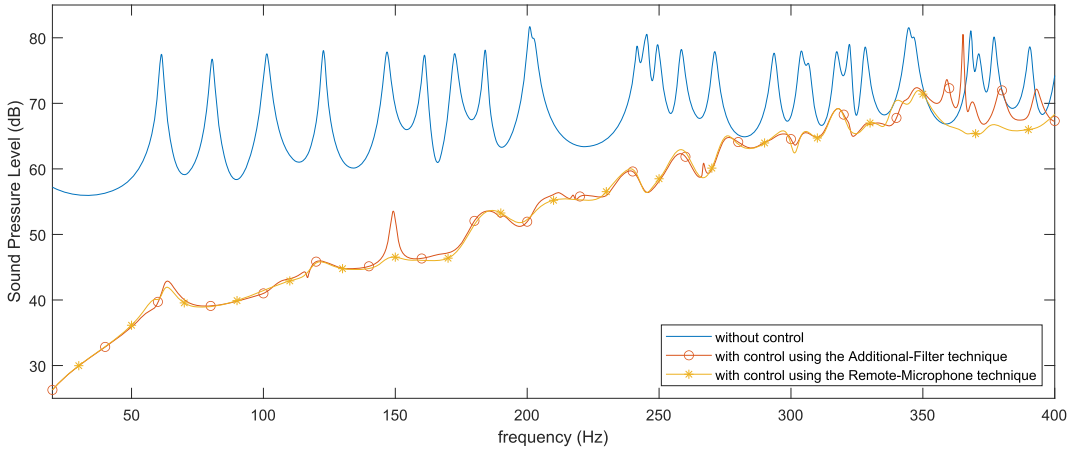

Figure 7. Spatial average of the RMS scattered acoustic pressure in the room measurement zone with control using the Remote-Microphone or the Additional-Filter technique.

only come directly from an acoustic source, but are already the result of previous reflections on other walls.

It can be concluded that the scattered pressure at any location close to the walls can be accurately estimated from total pressure measurements from a limited number of microphones, provided that measurements are taken on all the walls and not only around the estimation point.

5 Additional-Filter method vs. Remote-Microphone technique

The linear filtering of total pressure signals to obtain an estimate of a scattered pressure signal is analogous to the so-called RM technique for estimation of noise at virtual microphones [16]. A more recently proposed method for control at virtual microphones involves filtering not the signals on the real microphones, in order to generate minimization signals, but rather the control signals that minimize the real microphone signals. This so-called AF method has led in some cases to better results than the RM technique [17, 18]. It could be of interest in the case of the semi-anechoic room under study, because the number of sources is smaller than the number of microphones. The matrix to be identified at each frequency is therefore smaller with the AF, and could be obtained from data collected with a smaller number of reference source positions. As moving this heavy reference source around the room is by far the most tedious step in the whole control strategy studied here, we wanted to compare the RM and AF methods in 2D simulations of the semi-anechoic room.

If $\mathbf{U}_{\text{sca}}(\omega)$ and $\mathbf{U}(\omega)$ denote the matrix of control source signals which respectively minimize, for every position of the reference source, the scattered and total pressure at the microphones at angular frequency ω, instead of equation (6) the AF method relies on the computation $\mathbf{G}_{\text{AF}}$ which minimizes:

$$J_{\text{AF}} = ||\mathbf{U}_{\text{sca}}(\omega) - \mathbf{G}_{\text{AF}}(\omega)\mathbf{U}(\omega)||_{\text{Fro}}^2. \tag{8}$$

When an unknown primary source is radiating into the room, the sources signals to be used are computed by

filtering through $\mathbf{G}_{AF}$ the signals which minimize the total pressure signals.

Figure 7 shows the control simulation results obtained with each of the two methods when all the wall microphones are used for scattered field estimation with the configuration shown on the left of Figure 5. Up to 350 Hz, the AF technique leads to control results comparable to those obtained with the RM technique, at the exception of a few frequencies where the residual scattered pressure shows a small peak. These frequencies are close to the singular frequencies of the BPC device shown on the left of the Figure 5. At these frequencies, total pressure control is not a well-posed problem, and the use of additional filters does not make it better to achieve scattered pressure control. With the RM technique, the control of the estimated scattered pressure is also not well-posed but at least the estimation of the error signals is accurate. Beyond 350 Hz, the results of the AF technique are no longer acceptable. At these frequencies, the density of secondary sources is insufficient to enable global control of the scattered pressure in the room. The control signals are only capable of local minimization at the microphones, and the additional filter is no longer able to account for the underlying continuous operator, thereby preventing the mapping from real to scattered signals.

As AF tends to worsen the scattered field at higher frequencies, we decided to stick to the RM technique for the upcoming experiments at LMA.

6 Conclusions

The simulations presented in the paper have led to a number of practical results which have been directly incorporated into the design and construction of the active semi-anechoic room built at the LMA:

1. Microphone meshing of an irregular minimization surface seems to be sufficient in practice to overcome the theoretical singularity of BPC at the resonant frequencies of the volume bounded by the surface. This is far simpler and less expensive than using a double layer of microphones.

2. The estimation of the scattered pressure at one location based on total pressure measurements is, for comparable numbers of measurement points, significantly more accurate when these points cover the whole scattering surface rather than the vicinity of the estimation point.

3. In the case of the semi-anechoic room device considered here, control of the scattered pressure using RM technique seems to be more robust at the upper frequencies of interest than the AF method.

These results may also help the design of other set-ups for active control of scattered noise.

In conclusion the 2D simulations suggest that significant active reduction of the wall scattering may be achieved up to 250 Hz in the measurement zone of the LMA semi-anechoic room, provided one source and two microphones per meter are used close to the walls. Whereas control sources were monopoles in the 2D simulations, real life loudspeakers facing the walls may generate wavefronts more similar to the wall scattering and make control more global.

The experimental LMA set-up includes off-the-shelf loudspeakers with frequency cut-off around 100 Hz. Therefore in the experiment efficient control is expected in the 100–250 Hz range but not at lower frequencies.

At the time of writing, 3D numerical simulations have been performed and the LMA demonstration room has been equipped with loudspeakers and microphones, but no sound-absorbing material has been placed yet on the walls. Frequency Response Functions were measured in the room and used as a basis updating the Finite Element Model of the room, involving frequency-band wall impedances with higher sound absorption than in the 2D model used in this paper. Extensive testing of open-loop control of wall scattering and comparison with 3D numerical simulations are currently on the agenda. Real-time control in the room with absorbing material covering the walls is a longer-term prospect.

Acknowledgments

This work received support from the French government under the France 2030 investment plan, as part of the Initiative d'Excellence d'Aix-Marseille Université – A*MIDEX (AMX-19-IET-010).

Conflicts of interest

Author declared no conflict of interests.

Data availability statement

Data are available on request from the authors.

References

1. P. Nelson, S. Elliott: Active control of sound, Academic Press, London, 1992.
2. B. Kerferd, D. Eggler, M. Karimi, N. Kessissoglou: Active acoustic cloaking of cylindrical shells in low Mach number flow. Journal of Sound and Vibration 479 (2020) 115400. https://doi.org/10.1016/j.jsv.2020.115400.
3. C. House, J. Cheer, S. Daley: An experimental investigation into active structural acoustic cloaking of a flexible cylinder. Applied Acoustics 170 (2020) 107436. https://doi.org/10.1016/j.apacoust.2020.107436.
4. T.S. Becker, D.-J. van Manen, T. Haag, C. Bärlocher, X. Li, N. Börsing, A. Curtis, M. Serra-Garcia, J.O.A. Robertsson: Broadband acoustic invisibility and illusions. Science Advances 7, 37 (2021) eabi9627. https://doi.org/10.1126/sciadv.abi9627.
5. Y. Feng, X. Wang, M. Wu, J. Yang: Multizone active noise control for impulsive scattered sound of a rigid cylinder. Applied Acoustics 202 (2023) 109132. https://doi.org/10.1016/j.apacoust.2022.109132.
6. M. Mei, L. Zhang, B. An, J. Li: Approach to active control of scattered sound field from underwater targets. Journal of the Acoustical Society of America 154, 5 (2023) 2727–2745. https://doi.org/10.1121/10.0022049.
7. E. Friot: Control of low-frequency wall reflections in an anechoic room, in: ACTIVE 2006, Adelaide, Australia, 18–20 September, 2006.
8. D. Habault, E. Friot, P. Herzog, C. Pinhede: Active control in an anechoic room: theory and first simulations. Acta

Acustica united with Acustica 103, 3 (2017) 369–378. https://doi.org/10.3813/AAA.919066.
9. C. Pinhède, R. Boulandet, E. Friot, M.R. Allado, R. Côte, P. Herzog: Towards an active semianechoic room: simulations and first measurements, in: Forum Acusticum 2023, Torino, Italy, 11–15 September, 2023, https://doi.org/10.61782/fa.2023.0399.
10. R. Haasjes, A. Berkhoff: An efficient offline scheme to compute an FIR controller for active reduction of acoustic reflections in an anechoic chamber. Journal of Sound and Vibration 573 (2024) 118198. https://doi.org/10.1016/j.jsv.2023.118198.
11. E. Friot, C. Bordier: Real-time active suppression of scattered acoustic radiation. Journal of Sound and Vibration 278, 3 (2004) 563–580. https://doi.org/10.1016/j.jsv.2003.10.064.
12. E. Friot, R. Guillermin, M. Winninger: Active control of scattered acoustic radiation: A real-time implementation for a three-dimensional object. Acta Acustica united with Acustica 92 (2006) 278–288.
13. C. Pinhède, D. Habault, E. Friot, P. Herzog: Active control of the field scattered by the rigid wall of a semi-anechoic room–Simulations and full-scale offline experiment. Journal of Sound and Vibration 506 (2021) 116–134. https://doi.org/10.1016/j.jsv.2021.116134.
14. S. Takane, Y. Suzuki, T. Sone: A new method for global sound field reproduction based on Kirchhoff's integral equation. Acustica 85 (1999) 250–257.
15. N. Epain, E. Friot: Active control of sound inside a sphere via control of the acoustic pressure at the boundary surface. Journal of Sound and Vibration 299, 3 (2007) 587–604. https://doi.org/10.1016/j.jsv.2006.06.066.
16. A. Roure, A. Albarrarazin: The remote microphone technique for active noise control, in: INTER-NOISE and NOISE-CON Congress and Conference Proceedings, Active99, Fort Lauderdale, FL, 2–4 December, Institute of Noise Control Engineering, 1999, pp. 1233–1244.
17. J. Zhang, S.J. Elliott, J. Cheer: Robust performance of virtual sensing methods for active noise control. Mechanical Systems and Signal Processing 152 (2021) 107453. https://doi.org/10.1016/j.ymssp.2020.107453.
18. X. Cui, X. Wang, W. Yang, Z. Zhang, M. Wu, J. Yang: A robust design strategy for active control of scattered sound based on virtual sensing. Journal of the Acoustical Society of America 154, 4 (2023) 2539–2552. https://doi.org/10.1121/10.0021885.
19. R. Boulandet, M. Allado, C. Pinhède, E. Friot, R. Côte, P. Herzog: Simulation of a hybrid (passive/active) acoustic measurement room, in: COMSOL 2023 Conference, Munich, Germany, October 25–27, 2023.
20. C. Pinhède, P. Herzog: Design and measurement of a reference source at lower frequencies. Forum Acusticum 2020, Lyon, France, 2020.

Cite this article as: Friot E. Pinhède C. Herzog P. & Boulandet R. 2024. Optimizing a 2D active set-up for global control of low-frequency wall reflections in a semi-anechoic room. Acta Acustica, **8**, 68. https://doi.org/10.1051/aacus/2024077.